PAPER

Comparative analysis of the methods for quantitative determination of water content in skin from diffuse reflectance spectroscopy data

https://doi.org/10.1070/QEL17212

Comparative analysis of the methods for quantitative determination of water content in skin from diffuse reflectance spectroscopy data

B.P. Yakimov, D.A. Davydov, V.V. Fadeev, G.S. Budylin, E.A. Shirshin

Abstract. **The predictive properties of methods aimed for estimating the water content in skin from the spectral diffuse reflection characteristics near the water absorption line in the near-IR spectral range are analysed. Numerical simulation data, experimental data on diffuse reflection from human skin phantoms, and data from the reference data set of human skin reflectance spectra are used to consider the possibility of gaining additional information about the water distribution in skin. The influence of variations in the scattering coefficient and oxyhaemoglobin concentration on the water content estimates is investigated.**

Keywords: *diffuse reflectance, water absorption line, near-IR range, water content in skin.*

1. Introduction

Water, being the main component of a human body, is involved in numerous biochemical and biophysical processes occurring in human skin. Hydration of the upper layers of skin (*stratum corneum* and viable epidermis) is directly related to the aging processes [1] and skin sensitivity [2], whereas the water content in dermis correlates with the mechanical elasticity of skin [3]. Moreover, a change in the water concentration in tissues may also be a symptom of some serious diseases, e.g., chronic heart failure or impaired renal function [4]. Thus, the possibility of determining the water content in different skin layers is essential not only for dermatology needs but also for complex diagnostics of the functional state of patient.

Currently, it is impossible to select the best method for determining the water content in different skin layers. Despite the existence of several 'nonoptical' methods [5], optical measurements of water content in skin remain urgent because of their low invasiveness, short signal formation time, and small measurement error. Note also that the problem of determining water concentration is urgent not only for different skin sublayers. For example, it was shown in [6, 7] that the water content in tumour tissues exceeds significantly that in healthy tissues of oral cavity. This difference can be used for highly sensitive determination of tumour tissue boundaries in intraoperative diagnostics, which can be carried out using optical methods. In particular, Raman spectroscopy was applied in [6, 7] to find the water concentration (measurements at a frequency $\nu \approx 3400$ cm^{-1}) in healthy and pathological tissues.

Vibrational lines of water molecules manifest themselves not only in the Raman spectra but also in the absorption spectra of tissues in the near-IR range. In this study, we applied diffuse reflectance spectroscopy (DRS) to estimate the water content in skin. The spectrum of diffusely reflected radiation in the near-IR range is known to contain information about the fraction of photons absorbed by chromophores, thus making it possible to determine the chromophore concentrations in the studied object. However, since the problem of estimating absorption from diffuse reflectance spectra cannot be solved analytically in the general case, the chromophore concentrations are calculated from the DRS data using different approximations [8]. In the simplest case it is assumed that the optical sample density is determined by the logarithm of reflectance, and the chromophore concentrations are proportional to the difference in the optical densities at two wavelengths:

$$\mathrm{OD}(\lambda) = -\ln R(\lambda), \tag{1}$$

$$C \propto \mathrm{OD}(\lambda_1) - \mathrm{OD}(\lambda_2), \tag{2}$$

where $R(\lambda)$ is the diffuse reflectance at a wavelength λ, OD is the estimated optical density, and C is the chromophore concentration. The wavelengths λ_1 and λ_2 are generally chosen so as to correspond, respectively, to a local maximum and local minimum of chromophore absorption.

Most researchers use water absorption bands with local maxima at $\lambda = 1450$ nm (absorption coefficient $\mu_a \approx 30$ cm^{-1}) and 1920 nm ($\mu_a \approx 150$ cm^{-1}) to estimate the water content. These lines, which are overtones of the OH-bond vibration, are sensitive to small variations in water concentration in the upper layers of skin and make it possible to estimate the degree of hydration of the *stratum corneum* and viable epidermis. For example, the absorption bands at $\lambda = 1450$ and 1920 nm were used in [9–11] to visualise the skin moisture. The local maxima at $\lambda = 1190$ and 1450 nm were applied to monitor the dehydration of porcine skin during optical bleaching [12]. The absorption line at $\lambda = 1450$ nm was used in [13] to compare the DRS methods with the bioimpedance methods for estimating the epidermis moisture.

B.P. Yakimov, D.A. Davydov, V.V. Fadeev Faculty of Physics, Lomonosov Moscow State University, Vorob'evy gory, 119991 Moscow, Russia; **G.S. Budylin** Faculty of Physics, National Research University Higher School of Economics, ul. Myasnitskayaya 20, 101000 Moscow, Russia; **E.A. Shirshin** Faculty of Physics, Lomonosov Moscow State University, Vorob'evy gory, 119991 Moscow, Russia; Institute for Spectroscopy, Russian Academy of Sciences, ul. Fizicheskaya 5, Troitsk, 108840 Moscow, Russia; e-mail: shirshin@lid.phys.msu.ru

Received 27 November 2019
Kvantovaya Elektronika **50** (1) 41–46 (2020)
Translated by Yu.P. Sin'kov

The strong absorption ($\mu_a \approx 50$ cm^{-1}) in the range of 1400–2000 nm has some drawbacks; one of them is small light penetration depth (~ 100 μm) [14, 15], due to which the main contribution to the diffuse reflection spectrum is from the upper skin layers (mainly the *stratum corneum* and deeper lying epidermis layers). Quantitative determination of the degree of hydration of these layers is important for dermatology and cosmetology. At the same time, the determination of water content in deeper lying layers (dermis and hypodermic tissues) is also of interest, for example, for estimating the degree of edematous syndrome manifestation. One can record signals from deeper skin layers using a less intense water absorption band peaking at $\lambda = 980$ nm ($\mu_a \approx 0.5$ cm^{-1}) [16–18]. However, the consideration of several absorption lines to gain additional information about the water concentration profile in skin has not been analysed until now. The influence of a change in the concentration of other chromophores on the accuracy of algorithms for quantitative determination of water content has not been investigated either.

In this study we analysed several very simple algorithms for determining the water content in skin using water absorption bands at $\lambda = 980$, 1190, 1450, and 1920 nm for the diffuse reflectance spectra of human skin taken from the reference data set of the National Institute of Standards and Technologies (NIST, United States) and for the diffuse reflectance spectra simulated using the Monte Carlo method as applied to a homogeneous model of human skin. We estimated the errors of the water concentration determination algorithms that are introduced by scattering and variation in the concentration of haemoglobin, whose absorption spectrum is overlapped with the absorption spectrum of water in the range of 800–1000 nm. We also tested experimentally (using optical human skin phantoms) the possibility of determining the water content in skin from the intensity of water absorption band at $\lambda = 980$ nm.

2. Methods and materials

2.1. Algorithm testing

To estimate the errors of different methods for calculating the water content in skin, we used a reference data set of human skin reflectance (NIST, United States). This data set contains 100 averaged diffuse skin reflectance spectra measured for 100 volunteers in the range of 250–2500 nm in an optical configuration using an integrating sphere. The reflectance in this set is given in percentage of the incident light intensity. A complete description of the data can be found in [19].

Note that the analysis revealed nine spectra with a high melanin content (large OD values in the range of 600–700 nm). These spectra were rejected when estimating the errors of different techniques for calculating the water content in skin.

2.2. Numerical simulation

The values of skin diffuse reflectance R were calculated by modelling the light transport in skin using the Monte Carlo method (Monte Carlo modelling of light transport (MCML) [20]). Models with skin structure conceived in detail [21] and those without detailing the skin structure [22] are applied to solve clinical problems based on skin diffuse reflectance data. In this study the skin was modelled as a single-layer of a semi-infinite medium with constant absorption and scattering coefficients (μ_a and μ_s, respectively) and a fixed value of anisotropy factor g, which parameterises the Henyey–Greenstein scattering phase function. The choice of a homogeneous model, on the one hand, yields a rough estimate for a specific object. At the same time, it allows one to give up the discussion of morphological features and obtain a general qualitative concept about a wider class of objects, independent of their fine structural features. This model is also closer to that applied to describe skin using water content indices W.

Modelling was performed on a grid of parameters μ_a and μ_s; the coefficient μ_a was chosen to be in the range of 0.1–20 cm^{-1} (100 values on the logarithmic grid), the scattering coefficient μ_s was varied in the range of 100–2000 cm^{-1} (also 100 values on the logarithmic grid), and the anisotropy factor g was assumed to be constant: 0.9. Monte Carlo modelling was performed within a modified version of the GPU-MCML program [23], adapted for calculations on GPU-cluster nodes of the Lomonosov supercomputer [24].

2.3. Sample preparation

Fresh fragments of porcine ear skin 2 × 2 cm in size were used as human skin phantoms. These skin fragments reproduce both the morphological and molecular compositions of human skin and, correspondingly, have practically the same optical properties in the spectral range under consideration [25, 26]. For example, these phantoms are often applied to test cosmetic preparations for human skin barrier properties, using, in particular, optical techniques [27]. The samples were stored at a temperature of $T = 4$ °C to prevent them from natural dehydration. Their drying was performed at $T = 30$ °C–40 °C and normal pressure. Under these conditions, the changes in the sample mass corresponding to a change in the water concentration by 5% were observed after ~20 min of drying. The water concentration in the samples was calculated from the formula

$$C = \frac{m(t) - m_{\text{dry}}}{m(t)} 100\%, \tag{3}$$

where $m(t)$ is the sample mass at time t and m_{dry} is the mass of dry sample (after 40-h drying).

2.4. Schematic of the setup for measuring diffuse reflectance spectra

A specially developed experimental setup was used to determine the water content in phantom samples. This setup is based on a fibre transceiver composed of two water-free quartz fibres 600 μm in diameter, with a distance of 1 mm between the end face edges. Light from a halogen lamp (with a continuous emission spectrum in the range of 400–2500 nm) was introduced into one of the fibres, whereas the other fibre was connected to an input of Maya 2000Pro spectrometer (Ocean Optics, United States). The reference reflector was a mirror with a silver coating. The diffuse reflectance R was calculated from the formula

$$R = \frac{I - I_{\text{dark}}}{I_{\text{ref}} - I_{\text{dark}}}, \tag{4}$$

where I is the intensity of the sample signal measured by the spectrometer, I_{ref} is the reference reflector signal intensity, and I_{dark} is the spectrometer dark noise intensity.

3. Results

First of all, we analysed the mutual correlation between the water content indices W calculated using the data on several water absorption bands (at $\lambda = 980$, 1190, 1450, and 1920 nm) and reference points (at $\lambda = 850$, 1100, and 1300 nm). The water content indices W were found from the formula [9–12]

$$W(\lambda_1/\lambda_2) = \mathrm{OD}(\lambda_1) - \mathrm{OD}(\lambda_2), \quad (5)$$

where λ_1 and λ_2 are the wavelengths of the absorption band and baseline, respectively. This calculation method was applied in [9–12]. We used also the algorithm with subtraction of a straight line from the absorption, referenced to two local minima at $\lambda = 1280$ and 1650 nm, as was done in [13]. The water content indices were calculated for the spectra from the reference data set of human skin reflectance (NIST, United States). The averaged spectrum from this set and schematic diagrams clarifying the method for calculating water content indices are presented in Fig. 1a.

We found that the water content indices calculated using the absorption bands at $\lambda = 980$ and 1190 nm [W(980/850) and W(1190/1100)] correlate weakly with the values W(1450/1100) and W(1920/1100). At the same time, the indices W(1450/1100) and W(1920/1100), as well as W(1450), calculated with a linearly extrapolated baseline, are characterised by high ($r > 0.9$) cross-correlation coefficients (Figs 1b–1d).

The absence of correlations between the indices W calculated from different local absorption maxima may be due to two reasons. First, since the absorption coefficient of water at $\lambda = 980$ nm is an order of magnitude smaller than the absorption coefficients for other IR bands, identical changes in the scattering coefficients and concentrations of other chromophores, which also exhibit absorption in this spectral range, may lead to a larger relative error in estimating the water content from the band at $\lambda = 980$ nm. Second, the absence of correlations may be caused by inhomogeneous distribution of water concentration over different skin layers. Indeed, the water content in upper skin layers is known to be much lower than in deeper layers (~20 and ~70 wt%, respectively). Since the penetration depth of the radiation at $\lambda = 1450$ and 1920 nm is ~100 μm in the order of magnitude instead of ~2 mm for the radiation at $\lambda = 980$ nm, the diffuse reflectance signal is detected from different skin layers.

To verify the aforementioned hypotheses, the W values were calculated for diffuse reflectance spectra modelled by the Monte Carlo method. We generated two data sets with 100 spectra in each. Water concentration and scattering coefficient were varied in the first set, and the water and oxyhaemoglobin concentrations and scattering coefficient were simultaneously changed in the second set, whereas the concentrations of other components (deoxyhaemoglobin and melanin) remained constant. Figures 2a and 2b present examples of changes in the diffuse reflectance spectra with a change in the scattering coefficient and oxyhaemoglobin concentration, provided that the other parameters are constant. The spectrum of the skin scattering coefficient was taken from [15]; the scattering parameters were varied with deviation up to 10% from their means.

The spectra were calculated using the single-layer skin model with a layer thickness significantly exceeding the average light penetration depth; the chromophore distribution over the layer was assumed to be uniform. The water content for the simulated spectra was calculated using the

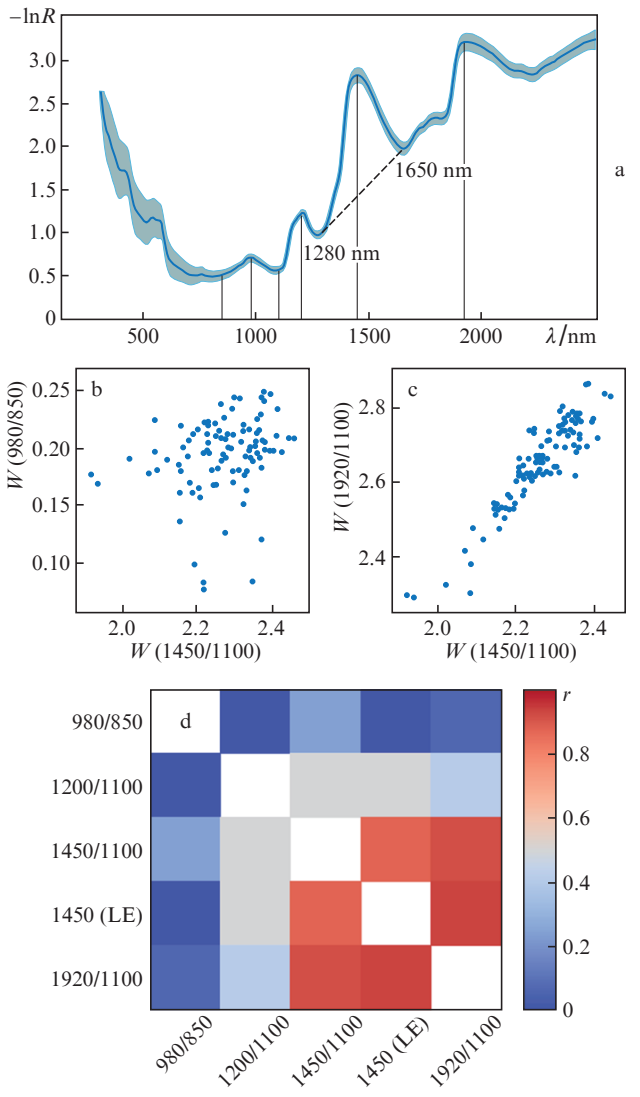

Figure 1. (Colour online) (a) Averaged spectrum and standard deviation of the optical density calculated using the NIST data set of human skin reflectance (vertical lines indicate the wavelengths used to calculate the water content indices W; the dashed line clarifies the procedure of spectrum correction using linear extrapolation (LE) of background); (b,c) two-dimensional scattering diagrams of indices W, calculated from different water absorption maxima (each point corresponds to one reflectance spectrum); and (d) a map of moduli of Pearson correlation coefficients r between the W values calculated using different water absorption bands.

methods applied for NIST data set. The W values were determined for the calculated spectra in the same way. Then the dependences of indices W on the water concentration embedded in the model were plotted (Fig. 2c). Correlation coefficients were calculated for these dependences; the most interesting values for two model series (with variable scattering coefficients and component concentrations) are presented in Fig. 2d.

One can see in Fig. 2d (blue columns) that the methods for calculating the water content using local absorption maxima at $\lambda = 1450$ and 980 nm have the same accuracy (estimated for r^2) for the first series of spectra. It was also found that the values W(1450/1100) and W(980/850) are mutually well correlated, being correlated with the water concentration value embedded in the model.

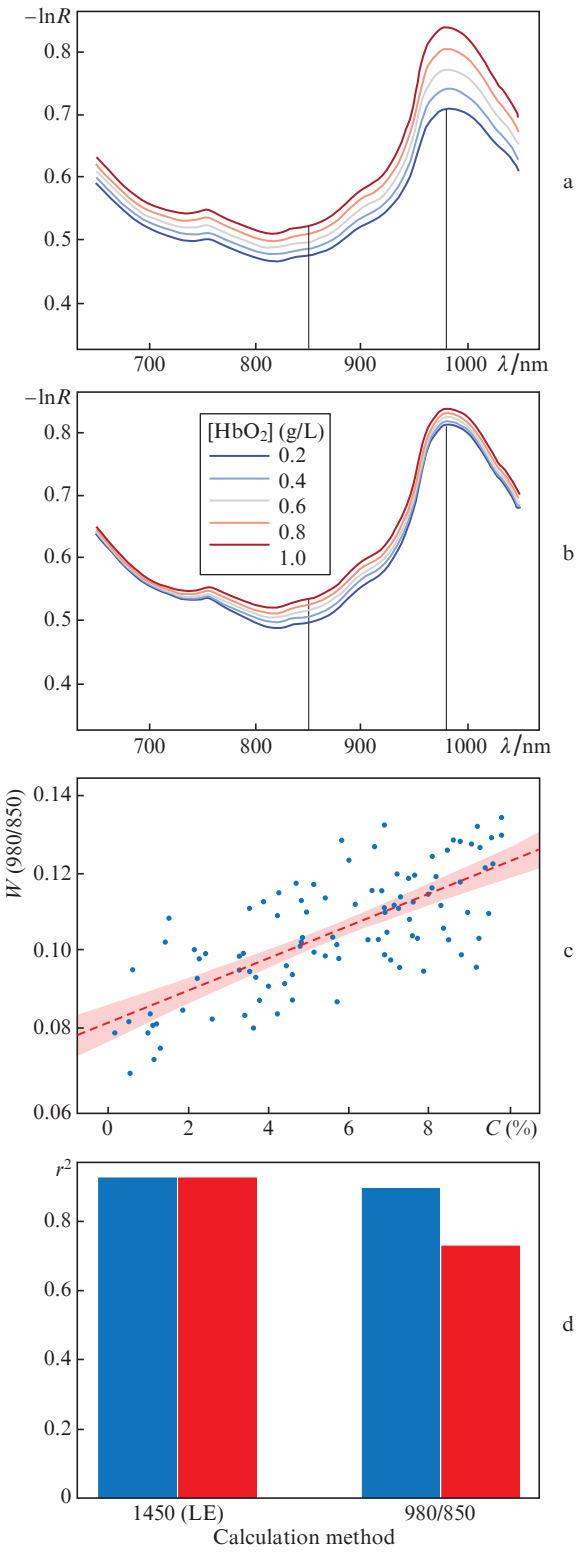

Figure 2. (Colour online) (a, b) Diffuse reflectance spectra simulated by the Monte Carlo method for different (a) scattering coefficients and (b) oxyhaemoglobin (HbO_2) concentrations; (c) correlation between the water content index calculated using the absorption band at $\lambda = 980$ nm and the true water concentration C specified when calculating model spectra; and (d) values of squared correlation coefficient, r^2, calculated for pairs of water concentrations (one embedded in the model spectrum and the other calculated using an estimation based on the index W) for two data sets, with simultaneous variation in the water concentration and scattering coefficient (blue columns) and the water and oxyhaemoglobin concentrations and scattering coefficient (red columns).

For the second generated data set, in which the scattering parameters and oxyhaemoglobin concentration were varied simultaneously with the water concentration, the accuracy of estimating the water content from the index $W(980/850)$ was poorer, whereas the accuracy of predicting the water content from $W(1450/1100)$ barely changed. Since the local maximum of the absorption band is overlapped with the long-wavelength absorption edge of oxyhaemoglobin, the $W(980/850)$ value may incorrectly correlate with the oxyhaemoglobin concentration, although the coefficient of this correlation is smaller than the correlation coefficient of $W(980/850)$ with the water concentration. Nevertheless, even in the case of variation in the scattering coefficient and haemoglobin concentration, the recovered water concentration correlates with the true concentration embedded in the model. Therefore, one can suggest the existence of correlation between the W values found from reflectance spectra at different wavelengths.

However, this correlation between the W indices for two wavelengths is not observed for the experimental spectra from the NIST data set. Based on this, one can conclude that the absence of correlation between the water concentrations estimated from experimental data using the W values for different wavelengths is explained by the absence of correlation between the real values of water concentration, related to the non-uniform water distribution in different skin layers.

Nevertheless, the modelling demonstrates the following: if the oxyhaemoglobin concentration remains constant, the water concentration in deep skin layers can be estimated based on very simple calculations of the water content index W for the absorption band at $\lambda = 980$ nm. This suggestion was verified experimentally on human skin phantoms. The latter were taken to be *ex vivo* porcine skin fragments, because their molecular and cellular composition practically coincides with that of human skin [25, 26]. To change the water concentration in phantom samples, they were dried at a temperature of 40 °C under normal pressure. Diffuse reflectance spectra were measured in the range of 500–1100 nm using a two-fibre scheme.

Figures 3a and 3b present diffuse reflectance and optical density spectra, estimated from the reflectance spectra using formula (1), for phantoms with different water concentrations. As can be seen in Fig. 3a, the amplitude of diffuse reflectance spectra changes significantly on average because of the changes in the scattering coefficient. Nevertheless, even with strong variation in the amplitude of reflectance spectra, one can clearly see a decrease in the local maximum of water absorption at $\lambda = 980$ nm (Fig. 3b).

One can clearly see in Fig. 3c that the $W(980/850)$ value depends on the water mass concentration in skin phantoms, calculated from formula (3). This dependence confirms the hypothesis that the water absorption band at $\lambda = 980$ nm can be used for quantitative estimation of the water content. Note that, along with oxyhaemoglobin, enhanced melanin content in skin may also affect the accuracy of determining the water concentration in skin based on the index $W(980/850)$. The influence of melanin was disregarded in our study: when analysing the NIST data set, these spectra were excluded from the sample, and the melanin concentration was assumed to be constant in modelling. Enhanced melanin content may indeed affect the quantitative estimation of water content. Nevertheless, when determining the water content, one can introduce a correction for the melanin content in skin using the data on its contribution to the diffuse reflectance spectrum in the wavelength range from 600 to 700 nm, as was done, for

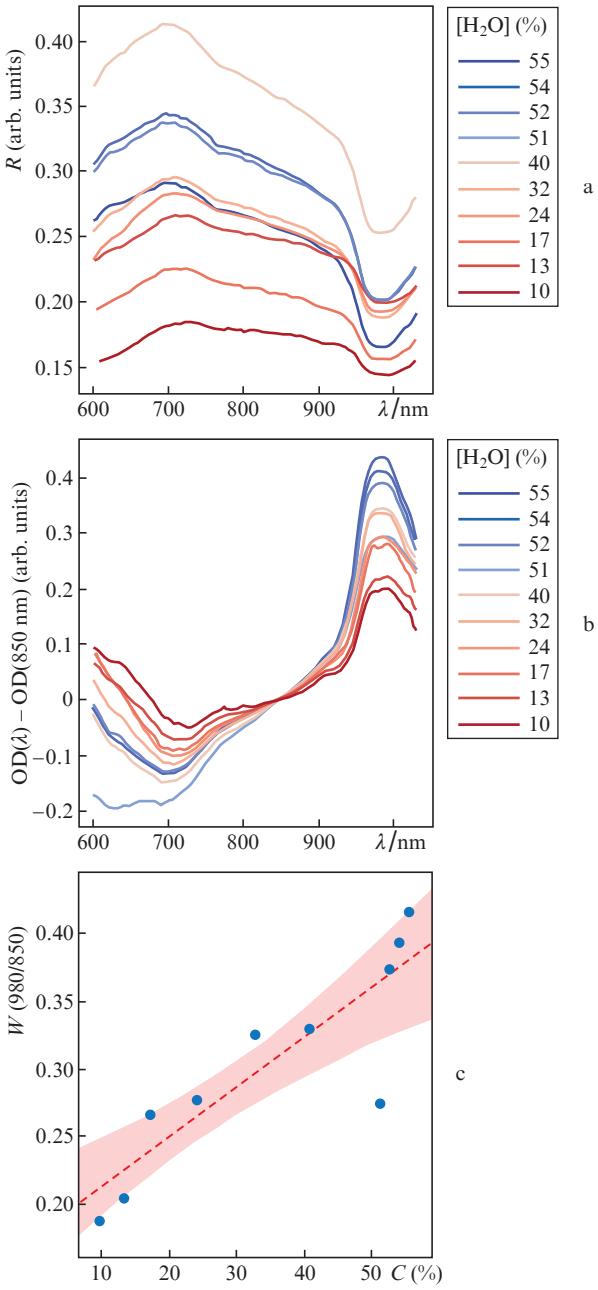

Figure 3. (Colour online) (a) Diffuse reflectance spectra of human skin phantoms with different water contents; (b) optical density spectra of skin phantoms with different water contents, corrected according to the baseline (λ = 850 nm); and (c) the dependence of water content index, calculated from the water absorption peak at λ = 980 nm, on the water mass concentration C in the phantoms, calculated from formula (3).

example, in [28] when determining the haemoglobin concentration in skin.

To verify the practical applicability of the method using the setup for measuring skin phantom spectra, we performed preliminary measurements of the dynamics of changes in the water concentration in deep skin layers using the water absorption line at λ = 980 nm (Fig. 4). The measurements were carried out for a sample of volunteers (ten people aged 19 to 25 years) during a 90-min cardio training. In the course of the experiment, diffuse reflectance spectra of the skin at the forearm inner side were measured for each participant prior to, during (45 min after the start), and after the training; fluid intake was not forbidden for the participants. The measurements were performed using the fibre probe described in Subsection 2.4; the distance between the fibre end faces was 2 mm. From three to four reflectance spectra were recorded in each measurement to average the values sought for.

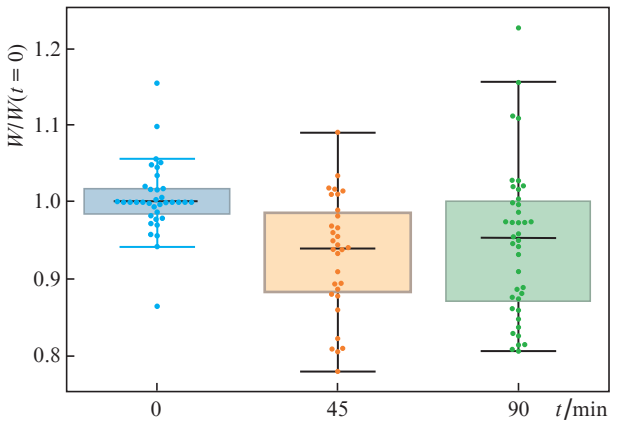

Figure 4. Values of the index W(980/850) for a group of volunteers during their training, normalised to the index measured before the training ($W(t = 0)$). The central horizontal lines correspond to the distribution medians, the horizontal sides of the rectangles correspond to the boundaries of the first and third distribution quartiles, and the horizontal upper and lower lines correspond to the one-and-a-half values of the interquartile peak-to-peak amplitude. Points are experimental W values.

The experimentally found W(980/850) values were significantly different for different volunteers. Therefore, to perform dynamics comparison, they were normalised to median W(980/850) values measured for each volunteer prior to training ($W(t = 0)$). It can be seen that the average relative water content in skin significantly decreases after physical loads. This decrease is most likely caused by the dehydration of deep skin layers as a result of physical loads. Furthermore, we are planning to perform larger-scale investigations of the dynamics of change in the skin water content during trainings and establish its correlations with the amount of total body water and degree of *stratum corneum* hydration.

4. Conclusions

The simplest algorithms for determining the water content in skin from diffuse reflectance spectroscopy data based on the open reference data set of human skin reflectance (NIST, United States) and numerically simulated diffuse reflectance spectra of the homogeneous skin model were compared. The water content estimates based on strong water absorption bands at λ = 1450 and 1920 nm were found to correlate weakly with the water content estimates based on the local absorption maximum at λ = 980 nm, which is due to the difference in the light penetration depths at the aforementioned wavelengths and the nonuniform distribution of water concentration over skin layers. It was also established that the quantitative estimate of water content based on the absorption line at λ = 980 nm is affected by changes in the oxyhaemoglobin concentration because of the superposition of oxyhaemoglobin and water absorption spectra in the range of 800–1000 nm. Nevertheless, the local maximum of water absorption at λ =

980 nm can be used to determine the water content in deep skin layers, as was experimentally confirmed for human skin phantoms.

The experiment with volunteers, performed on the basis of the above-described technique, indicates that this technique can be used to monitor the water content in tissues during trainings and under other intense physical loads in order to prevent organism from dehydration. Other possible fields of application of this method for estimating water content are monitoring of the state of patients with heart failure, which is generally accompanied by the development of oedematous syndrome, monitoring of patients' state when carrying out infusions, and estimation of the cosmetic state of skin.

Acknowledgements. The research is carried out using the equipment of the shared research facilities of HPC computing resources at Lomonosov Moscow State University. This study was supported by the Russian Science Foundation (Grant No. 18-15-00422) and the RF President's Foundation for State Support of Young Russian Scientists (Grant No. MK-2999.2019.2).

References

1. Choe C., Schleusener J., Lademann J., Darvin M.E. *Mech. Ageing Dev.*, **172**, 6 (2018).
2. Farage M.A., Katsarou A., Maibach H.I. *Contact Dermatitis*, **55**, 1 (2006).
3. Waller J.M., Maibach H.I. *Skin Res. Technol.*, **12**, 145 (2006).
4. Cho S., Atwood J.E. *Am. J. Med.*, **113**, 580 (2002).
5. Asogwa C., Lai D. *Electronics*, **6**, 82 (2017).
6. Barroso E., Smits R., Bakker Schut T., Ten Hove I., Hardillo J., Wolvius E., Baatenburg de Jong R.J., Koljenović S., Puppels G. *Anal. Chem.*, **87**, 2419 (2015).
7. Barroso E.M., Smits R.W., van Lanschot C.G., Caspers P.J., Ten Hove I., Mast H., Sewnaik A., Hardillo J.A., Meeuwis C.A., Verdijk R. *Cancer Res.*, **76**, 5945 (2016).
8. Tuchin V.V. *Opticheskaya biomeditsinskaya diagnostika* (Optical Biomedical Diagnostics) (Moscow: Fizmatlit, 2007) Vol. 1, p. 560.
9. Iwasaki H., Miyazawa K., Nakauchi S. *Proc. SPIE*, **6062**, 606203 (2006).
10. Egawa M., Yanai M., Kikuchi K., Masuda Y. *Appl. Spectrosc.*, **65**, 924 (2011).
11. Egawa M., Yanai M., Maruyama N., Fukaya Y., Hirao T. *Appl. Spectrosc.*, **69**, 481 (2015).
12. Yu T., Wen X., Luo Q., Zhu D., Tuchin V.V. *J. Biomed. Opt.*, **16**, 095002 (2011).
13. Saknite I., Zavorins A., Zablocka I., Kisis J., Spigulis J. *J. Biomed. Photonics Eng.*, **3**, 010310 (2017).
14. Arimoto H., Egawa M., Yamada Y. *Skin Res. Technol.*, **11**, 27 (2005).
15. Bashkatov A., Genina E., Kochubey V., Tuchin V. *J. Phys. D: Appl. Phys.*, **38**, 2543 (2005).
16. Stamatas G.N., Southall M., Kollias N. *J. Invest. Dermatol.*, **126**, 1753 (2006).
17. Chung S., Cerussi A., Klifa C., Baek H., Birgul O., Gulsen G., Merritt S., Hsiang D., Tromberg B. *Phys. Med. Biol.*, **53**, 6713 (2008).
18. Chung S.H., Yu H., Su M.-Y., Cerussi A.E., Tromberg B.J. *J. Biomed. Opt.*, **17**, 071304 (2012).
19. Cooksey C., Allen D.W., Tsai B.K. *NIST J. Res.*, **122**, N26 (2017).
20. Wang L., Jacques S.L., Zheng L. *Comput. Methods Programs Biomed.*, **47**, 131 (1995).
21. Zherebtsov E., Dremin V., Popov A., Doronin A., Kurakina D., Kirillin M., Meglinski I., Bykov A. *Biomed. Opt. Express*, **10**, 3545 (2019).
22. Tzeng S.-Y., Guo J.-Y., Yang C.-C., Hsu C.-K., Huang H.J., Chou S.-J., Hwang C.-H., Tseng S.-H. *Biomed. Opt. Express*, **7**, 616 (2016).
23. Alerstam E., Svensson T., Andersson-Engels S. *J. Biomed. Opt.*, **13**, 060504 (2008).
24. Sadovnichy V., Tikhonravov A., Voevodin V., Opanasenko V., in *Contemporary High Performance Computing* (Boca-Raton: CRC, 2017) pp 283–307.
25. Darvin M.E., Richter H., Zhu Y.J., Meinke M.C., Knorr F., Gonchukov S.A., Koenig K., Lademann J. *Quantum Electron.*, **44**, 646 (2014) [*Kvantovaya Elektron.*, **44**, 646 (2014)].
26. Du Y., Hu X., Cariveau M., Ma X., Kalmus G., Lu J. *Phys. Med. Biol.*, **46**, 167 (2001).
27. Choe C., Schleusener J., Lademann J., Darvin M.E. *J. Biophotonics*, **11**, e201700355 (2018).
28. Dolotov L., Sinichkin Yu.P., Tuchin V., Utz S., Altshuler G., Yaroslavsky I. *Lasers Surg. Med.*, **34**, 127 (2004).